Comparison of feedback strategies for noise suppression in protein level

Madeline Smith[1], Khem Raj Ghusinga[2], and Abhyudai Singh[3]

***Abstract*— Stochastic variation in the level of a protein among cells of the same population is ubiquitous across cell types and organisms. These random variations are a consequence of low-copy numbers, amplified by the characteristically probabilistic nature of biochemical reactions associated with gene-expression. We systematically compare and contrast negative feedback architectures in their ability to regulate random fluctuations in protein levels. Our stochastic model consists of gene synthesizing pre-mRNAs in transcriptional bursts. Each pre-mRNA transcript is exported to the cytoplasm and is subsequently translated into protein molecules. In this setup, three feedbacks architectures are implemented: protein inhibiting transcription of its own gene (I), protein enhancing the nuclear pre-mRNA decay rate (II), and protein inhibiting the export of pre-mRNAs (III). Explicit analytic expressions are developed to quantify the protein noise levels for each feedback strategy. Mathematically controlled comparisons provide insights into the noise-suppression properties of these feedbacks. For example, when the protein half-life is long, or the pre-mRNA decay is fast, then feedback architecture I provides the best noise attenuation. In contrast, when the timescales of export, mRNA, and protein turnover are similar, then III is superior to both II and I. We finally discuss biological relevance of these findings in context of noise suppression in an HIV cell-fate decision circuit.**

I. INTRODUCTION

Random variability in protein levels among a homogeneous cell population is referred to as gene-expression noise. This variability arises due to the characteristically probabilistic biochemical reactions associated with gene-expression and the low copy numbers of the species involved [1], [2]. Prevalence of noise in gene-expression suggests that cells must have mechanisms to cope with it, suppress it, or even utilize it to their advantage [3]–[14].

In this work, we are specifically interested in strategies that suppress the noise in gene-expression. Many prior studies have investigated feedback control strategies, wherein a protein self-regulates its own production, as mechanisms of noise suppression [15]–[23]. However, these models tend to exclusively consider feedback at the transcriptional or translational level, while failing to investigate feedback loops at the precursor mRNA level. Recent work indicates that feedback at the pre-mRNA level can play an important role in noise suppression [24]–[29]. Therefore, we incorporate different feedback loops in a model that includes retention of pre-mRNAs in the nucleus. We explore three different forms of negative feedback. The noise suppression abilities of each feedback mechanism are quantified, and then compared and contrasted.

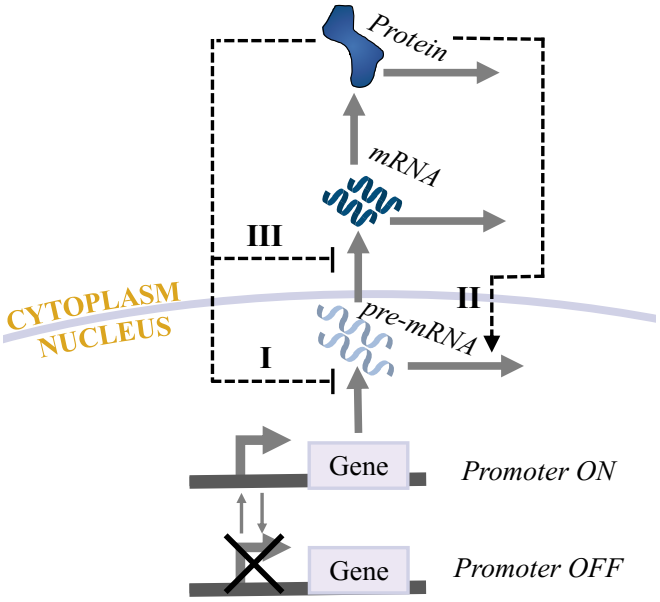

Fig. 1: Process of gene-expression modeled by precursor mRNA produced in transcriptional bursts inside the nucleus from the active gene promoter. Precursor mRNA is spliced and exported out of the nucleus as functional mRNA, and finally translated into protein. Proposed feedback mechanisms affecting pre-mRNA transcription (I), decay (II), or export (III) are depicted as dashed lines. The arrow head denotes activation, while the flat arrow denotes inhibition.

We describe gene-expression in the cells nucleus where the promoter produces a burst of multiple pre-mRNAs. Modeling transcription by bursting allows incorporation of the active (ON) and inactive (OFF) intervals of promoter activity [30], [30]–[38]. Next, the pre-mRNA is spliced and exported from the nucleus as functional mRNA. It is then translated and encodes a single protein. The three feedback architectures that we study are implemented in this model as follows:

I: the protein inhibits transcription of its own gene,
II: the protein enhances the nuclear pre-mRNA decay rate, and
III: the protein inhibits the export of pre-mRNAs.

We compare and contrast the noise suppression abilities of these three models in a mathematically controlled fashion [39]. To that end, the mean level of protein is kept constant

[1]Madeline Smith is an undergraduate student in the Department of Bio-medical Engineering, University of Delaware, Newark, DE, USA. smithmad@udel.edu

[2]Khem Raj Ghusinga is a PhD student in the Department of Electrical and Computer Engineering, University of Delaware, Newark, DE, USA. khem@udel.edu

[3]Abhyudai Singh is with the Faculty of Electrical and Computer Engineering, University of Delaware, Newark, DE, USA. absingh@udel.edu

among all architectures. We find that when the protein half-life is long, or the pre-mRNA decay is fast, then feedback architecture I provides the best noise attenuation. In contrast, when the timescales of export, mRNA, and protein turnover are similar, then III is superior to both II and I.

The paper is organized as follows. Section II introduces the gene-expression model and resulting moment dynamics used to quantify the protein noise levels. Feedback strategies are incorporated and noise equations are obtained in Section III. Next, Section IV provides stability analysis of each feedback architecture. In Section V, we compare and contrast noise suppression of feedback architectures I-III under different regimes. A discussion of biological relevance of these findings in context of the role noise suppression plays in an HIV cell-fate decision concludes the work in Section VI.

II. GENE-EXPRESSION MODEL WITH NO REGULATION

We model gene-expression starting with nuclear pre-mRNA transcripts produced in bursts. Transcriptional bursting at the gene promoter occurs at a rate of k_r, creating B number of pre-mRNA transcripts, where B is drawn from a positive-valued distribution. The pre-mRNA is spliced and exported out of the nucleus at a rate of k_m to become functional mRNA, which is then translated into proteins at a rate k_p. Other parameters of the model include the degradation rate of pre-mRNA (γ_r), degradation rate of mRNA (γ_m), and degradation rate of protein (γ_p).

TABLE I: Frequency of gene-expression events and corresponding reset map.

Event	**Reset in Population Count**	**Probability Event will Occur in** $(t, t+dt)$
Transcriptional Bursting	$r(t) \to r(t) + B$	$k_r dt$
pre-mRNA Degradation	$r(t) \to r(t) - 1$	$\gamma_r r(t) dt$
pre-mRNA Export	$m(t) \to m(t) + 1$	$k_m r(t) dt$
mRNA Degradation	$m(t) \to m(t) - 1$	$\gamma_m m(t) dt$
Protein Translation	$p(t) \to p(t) + 1$	$k_p m(t) dt$
Protein Degradation	$p(t) \to p(t) - 1$	$\gamma_p p(t) dt$

Let $r(t)$, $m(t)$, and $p(t)$ represent the count of pre-mRNA, mRNA, and protein molecules at time t, accordingly. The probabilities of occurrences of these events in an infinitesimal time-interval $(t, t+dt)$ are described in Table 1. Only a single event, other than the bursts, can occur at a time and with each event that occurs, the count of each state $r(t)$, $m(t)$, and $p(t)$ are reset.

To quantify the noise in protein levels of the gene-expression model, we write differential equations for time evolution of the statistical moments. For the gene-expression model without feedback, time derivative of the expected value of a differentiable function $\varphi(r, m, p)$ is given by [40], [41]

$$\begin{aligned}\frac{d\langle\varphi(r,m,p)\rangle}{dt} = \Big\langle & k_r[\varphi(r+B,m,p)-\varphi(r,m,p)] \\ & + \gamma_r r[\varphi(r-1,m,p)-\varphi(r,m,p)] \\ & + k_m r[\varphi(r-1,m+1,p)-\varphi(r,m,p)] \\ & + \gamma_m m[\varphi(r,m-1,p)-\varphi(r,m,p)] \\ & + k_p m[\varphi(r,m,p+1)-\varphi(r,m,p)] \\ & + \gamma_p p[\varphi(r,m,p-1)-\varphi(m,p)]\Big\rangle.\end{aligned} \tag{1}$$

Here, and for the remainder of the paper, $\langle . \rangle$ is used to represent the expected value. Choosing appropriate functions for φ gives the following moment dynamics:

$$\begin{aligned}\frac{d\langle r\rangle}{dt} &= k_r\langle B\rangle - (k_m+\gamma_r)\langle r\rangle \\ \frac{d\langle m\rangle}{dt} &= k_m\langle r\rangle - \gamma_m\langle m\rangle \\ \frac{d\langle p\rangle}{dt} &= k_p\langle m\rangle - \gamma_p\langle p\rangle \\ \frac{d\langle r^2\rangle}{dt} &= k_r\langle B^2\rangle - 2(k_m+\gamma_r)\langle r^2\rangle \\ &\quad + (k_m + 2\langle B\rangle k_r + \gamma_r)\langle r\rangle \\ \frac{d\langle m^2\rangle}{dt} &= (k_m + 2k_m\langle m\rangle)\langle r\rangle + \gamma_m\langle m\rangle \\ &\quad - 2\gamma_m\langle m^2\rangle \\ \frac{d\langle p^2\rangle}{dt} &= (k_p + 2k_p\langle p\rangle)\langle m\rangle + \gamma_p\langle p\rangle \\ &\quad - 2\gamma_p\langle p^2\rangle \\ \frac{d\langle rm\rangle}{dt} &= k_r\langle B\rangle\langle m\rangle + k_m\langle r^2\rangle \\ &\quad + \langle r\rangle(-k_m + \langle m\rangle(-k_m-\gamma_m-\gamma_r)) \\ \frac{d\langle rp\rangle}{dt} &= k_r\langle B\rangle\langle p\rangle + \langle r\rangle(k_p\langle m\rangle \\ &\quad + \langle p\rangle(-k_m-\gamma_p-\gamma_r)) \\ \frac{d\langle mp\rangle}{dt} &= k_p\langle m^2\rangle + k_m\langle p\rangle\langle r\rangle \\ &\quad - \langle m\rangle\langle p\rangle(\gamma_m+\gamma_p).\end{aligned} \tag{2}$$

The steady-state moments can be computed from the above moment dynamics equations by equating each of them to zero. We are particularly interested in studying the noise in protein level, which is quantified via the coefficient of variation squared (CV^2, variance divided by squared of the mean). We also introduce two new parameters that allow simplification:

$$f = \frac{k_m}{\gamma_r}, \quad B_e = \frac{\langle B^2\rangle - \langle B\rangle}{2\langle B\rangle}. \tag{3}$$

Here, f represents a fixed ratio of pre-mRNA export from the nucleus and pre-mRNA degradation, which is kept constant during analysis, and B_e relates to the transcriptional burst size of pre-mRNA.

Solving (2) for steady-state moments, and substituting the above parameters yields

$$CV^2 = \frac{1}{\langle \bar{p} \rangle} + \frac{\gamma_p(\gamma_m\gamma_p + (\gamma_r(\gamma_m + \gamma_p) + \gamma_r^2(1+f))(1+f+B_e f))}{(\gamma_m+\gamma_p)(\gamma_r+\gamma_m+\gamma_r f)(\gamma_r+\gamma_p+\gamma_r f)\langle \bar{m} \rangle}. \tag{4}$$

where $\langle \bar{p} \rangle = \langle \bar{m} \rangle k_p / \gamma_p$ is the steady-state mean protein level. Note that in (4), the first term is the intrinsic Poissonian noise due to stochastic births and deaths of single protein molecules. This term can be ignored when considering the order of magnitude size difference in population counts of mRNA and protein ($\langle \bar{m} \rangle / \langle \bar{p} \rangle$) $\approx 10^{-3}$ [2]. In such a case, the noise in protein levels depends inversely on the average steady-state level of mRNA $\langle \bar{m} \rangle$. The simplified coefficient of variation squared in the center column of Fig. 2 represents the noise at the protein level of the gene expression model with no feedback.

We next explore the noise expression of this model in different limits. For fixed f and very fast pre-mRNA decay (γ_r), the equation simplifies to:

$$\lim_{\gamma_r \to \infty} CV^2 = \frac{\gamma_p(1+f+B_e f)}{(\gamma_m+\gamma_p)(1+f)\langle \bar{m} \rangle}. \tag{5}$$

When the export of pre-mRNA (f) is very fast, the equation simplifies to:

$$\lim_{f \to \infty} CV^2 = \frac{(1+B_e)\gamma_p}{(\gamma_m+\gamma_p)\langle \bar{m} \rangle}. \tag{6}$$

However, when the export rate (f) is very slow, the equation then simplifies to:

$$\lim_{f \to 0} CV^2 = \frac{\gamma_p}{(\gamma_m+\gamma_p)\langle \bar{m} \rangle}. \tag{7}$$

Thus, regimes of either fast pre-mRNA decay or fast export result in an increasing relationship of noise and transcriptional burst size (5,6), while the noise in the case of slow export unaffected by transcriptional burst size (7). In all regimes, there is an inverse relationship of mRNA count and noise.

III. INTRODUCING REGULATORY MECHANISMS IN GENE-EXPRESSION

Here, we implement three different feedback loops and systematically compare their abilities to suppress noise. Feedback is incorporated by no longer assuming that the rate being regulated is fixed and constant (as described in Table I), but instead assuming that it is either a monotonically increasing or decreasing function of protein count. We perform this procedure for each feedback loop, as depicted in Fig. 1. To allow computation of comparable noise expressions, the protein dependant rates are then quantified by *linear noise approximation*. This involves linearizing the rate about the steady-state average protein count $\langle \bar{p} \rangle$ [42]. Note, these assumptions are only valid for small fluctuations in protein counts. This holds as regulatory protein levels in cells are tightly maintained within certain bounds. After linearizing the protein dependant rate, the new term is then substituted into the differential equations and it replaces the original constant rate associated with the gene-expression model without regulation in (1). The new time evolution and corresponding moment dynamics are obtained for each feedback architecture respectively.

A. Protein-Mediated Transcriptional Bursting Inhibition

First, we model transcriptional bursting regulation, depicted as feedback architecture I in Fig. 1, by assuming that transcriptional bursting events occur as a monotonically decreasing function $k_r(p)$ of the protein count $p(t)$. This results in a negative feedback strategy where an increase (decrease) in protein count will result in a decrease (increase) in bursting. Following the convention in [22], the rate $k_r(p)$ is linearized about the steady-state average number of protein $\langle \bar{p} \rangle$ and we assume

$$k_r(p) \approx k_r(\langle \bar{p} \rangle)\Big[1 - \varepsilon\Big(\frac{p(t) - \langle \bar{p} \rangle}{\langle \bar{p} \rangle}\Big)\Big] \tag{8}$$

with an average transcription rate of $k_r(\langle \bar{p} \rangle)$. The dimensionless constant

$$\varepsilon = -\frac{\langle \bar{p} \rangle}{k_r(\langle \bar{p} \rangle)} \frac{dk_r(p)}{dp} \tag{9}$$

corresponds to the sensitivity of the transcription rate to changes in $p(t)$ [22]. In simpler terms, this represents the strength of the feedback.

B. Protein-Mediated Enhancement of pre-mRNA Decay

Next, regulation by protein enhancement of pre-mRNA decay, feedback architecture II described in Fig. 1, is incorporated into the model. In this feedback strategy, pre-mRNA degrades at a rate of $\gamma_r(p)$. This form of regulation is not only dependent on protein count $p(t)$, but also on the count of pre-mRNA $r(t)$, resulting in a more complex form of feedback. We model this by $\gamma_r(p)r$ that is assumed to be a monotonically increasing function of protein count $p(t)$. The approximated rate $\gamma_r(p)r$ is linearized around both the average pre-mRNA count $\langle \bar{r} \rangle$ and protein count $\langle \bar{p} \rangle$. Again, it is assumed that $r(t)$ and $p(t)$ are tightly regulated and have small fluctuations from their respective steady-state averages. We find

$$\gamma_r(p)r \approx \gamma_r(\langle \bar{p} \rangle)\Big[r(t) + \langle \bar{r} \rangle \varepsilon\Big(\frac{p(t) - \langle \bar{p} \rangle}{\langle \bar{p} \rangle}\Big)\Big] \tag{10}$$

as the average pre-mRNA degradation rate $\gamma_r(\langle \bar{p} \rangle)r$ and dimensionless constant:

$$\varepsilon = \frac{\langle \bar{p} \rangle}{\gamma_r(\langle \bar{p} \rangle)} \frac{d\gamma_r(p)}{dp} \tag{11}$$

that is the sensitivity of the degradation rate to change in $p(t)$.

C. Protein-Mediated Inhibition of pre-mRNA Export

Last, we consider regulation of the export of pre-mRNA from the cell nucleus to the cytoplasm, depicted as feedback architecture III in Fig. 1. Here, we assume that export is a monotonically decreasing function based of protein count, but is also dependant on the count of pre-mRNA. The total export rate $k_m(p)r$ is dependant on both $p(t)$ and $r(t)$. The linear approximation of $k_m(p)r$ about $\langle\bar{r}\rangle$ and $\langle\bar{p}\rangle$ assumes that $r(t)$ and $p(t)$ are tightly regulated and have small fluctuations from their steady state averages. The total conversion rate can be approximated as:

$$k_m(p)r \approx k_m(\langle\bar{p}\rangle)\Big[r(t) - \langle\bar{r}\rangle\varepsilon\Big(\frac{p(t)-\langle\bar{p}\rangle}{\langle\bar{p}\rangle}\Big)\Big] \tag{12}$$

with an average degradation rate of $k_m(\langle\bar{p}\rangle)r$ and dimensionless constant of

$$\varepsilon = -\frac{\langle\bar{p}\rangle}{k_m(\langle\bar{p}\rangle)}\frac{dk_m(p)}{dp} \tag{13}$$

that corresponds to the negative feedback strength.

The time evolution of the statistical moments of each feedback mechanism are obtained by substituting the corresponding average rate found by linear approximation for the original rate in (1). This results in a unique solution of moment dynamics for each feedback architecture I-III. Based on the moment dynamics, the resulting protein noise levels of each feedback architecture is quantified as $CV_X^2, X\epsilon$ {I, II, III} and displayed in the middle row of Fig. 2. Note that in the remainder of the paper, $CV_X^2, X\epsilon$ {I, II, III} denotes the coefficient of variation squared of architecture X. Additionally, when there is no feedback strength, $\varepsilon = 0$, the resulting noise expressions correspond to the protein level noise when there is no feedback present $CV_X^2 = CV^2$.

IV. STABILITY ANALYSIS

A close examination of the gene-expression noise equations in Fig. 2 reveals that noise can become unbounded for some values of feedback strength (ε). Here, we find the conditions that result in bounded noise when feedback regulation is included in the model and analyze noise behavior under changing parameters.

A system is considered stable if the roots of its "real polynomial" (P) lie in the left half plane of the complex plane. The systems presented in this paper have three states that can be represented by a third-order polynomial, given by:

$$A = x^3 + ax^2 + bx + c. \tag{14}$$

The polynomial (A) is stable, and thus a stable system, when A is greater than 0. This is true when the following conditions are met:

$$a > 0, b > 0, 0 < c < ab. \tag{15}$$

We can describe feedback architecture I by the following square matrix A.

$$A = \begin{bmatrix} -\gamma_r - k_m & 0 & -\frac{B\varepsilon k_r}{\langle\bar{p}\rangle} \\ k_m & -\gamma_m & 0 \\ 0 & \frac{\gamma_p\langle\bar{p}\rangle}{\langle\bar{m}\rangle} & -\gamma_p \end{bmatrix}$$

Next, the characteristic polynomial is obtained to ultimately find a, b, and c. Feedback architecture I has a characteristic polynomial given by:

$$= -\frac{(-\gamma_m\gamma_p\varepsilon k_m(\gamma_r+k_m)+k_m(-\gamma_m-x)(\gamma_r+x)(\gamma_r+k_m+x))\langle\bar{m}\rangle\langle\bar{p}\rangle}{(k_m\langle\bar{m}\rangle\langle\bar{p}\rangle)}$$

and the following corresponding roots:

$$\begin{aligned} a &= \gamma_r(\gamma_m+\gamma_p) + \gamma_p k_m + \gamma_m(\gamma_p + k_m) \\ b &= \frac{1}{2}(2(\gamma_r+\gamma_m+\gamma_z+k_m) \\ c &= \gamma_m\gamma_p(1+\varepsilon)(\gamma_r+k_m) \end{aligned} \tag{16}$$

Based on the above values for a, b, and c, we find that the following condition for stability:

$$0 < c < ab \tag{17}$$

is only met when the following condition of feedback strength (ε) is met:

$$\varepsilon \leq \frac{(\gamma_m+\gamma_p)(\gamma_r+\gamma_m+k_m)(\gamma_r+\gamma_p+k_m)}{\gamma_m\gamma_p(\gamma_r+k_m)} \tag{18}$$

The above procedure is additionally performed in the same manner for feedback architectures II and III. We find that feedback II is stable for the same conditions as found above (same stability as feedback architecture I) (18). These stable and unstable regions of feedback architectures I and II are illustrated in relation to corresponding values of feedback strength (ε) and protein decay rate (γ_p) in Fig. IV. This figure also displays the region of stability when the mRNA decay rate is altered (γ_m). The region of stability is much smaller for low values of γ_m, but the system exhibits a greater region of stability when mRNA decays very fast. Additionally, the stability analysis of protein regulation of pre-mRNA export (feedback architecture III) results in a stable system for all values of feedback strength ε.

V. COMPARISON BETWEEN FEEDBACK STRATEGIES

Mathematically controlled comparisons are performed to determine which architecture best attenuates noise. These comparisons are controlled by assuming all steady-state average values to be the same among the three feedback strategies.

The first observation is made by comparing noise attenuation when the pre-mRNA degradation rate (γ_r) is considered to be very fast. In this limit, the ratio of pre-mRNA export and pre-mRNA degradation is kept constant. The resulting analytical noise expressions while approaching this limit can be found in the third column of Fig. 2. When comparing transcriptional regulation to regulation of pre-mRNA decay, we find that:

$$\lim_{\gamma_r\to\infty}\frac{CV_I}{CV_{II}} = \frac{1+\epsilon+f}{1+\epsilon+f+f\epsilon} < 1. \tag{19}$$

This indicates that under the regime of very fast pre-mRNA degradation, feedback architecture I is always better than II, regardless of feedback strength. However, when comparing

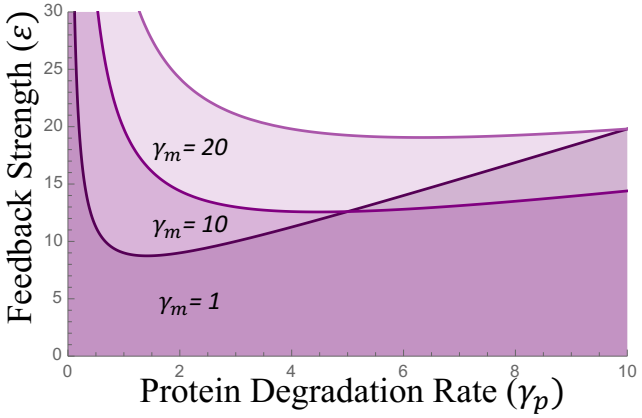

Fig. 3: Depiction of stability analysis of feedback architectures I and II. The system will remain stable for values of feedback strength (ε) and protein degradation rates (γ_p) that fall within the shaded region. For combinations of these parameters that fall above the shaded region, the noise will become unbounded and unstable. The darkest shade depicts the stable region when mRNA decay γ_m is equal to 1, the middle shade correlates to the stable region when γ_m = 10, and the lightest shaded region correlates to the stable region when γ_m = 20. The remaining parameters include: k_m = 1 and γ_r = 1.

regulation of pre-mRNA decay rate to regulation of pre-mRNA export rate, the following result is found:

$$\lim_{\gamma_r \to \infty} \frac{CV_{III}}{CV_{II}} = 1. \tag{20}$$

Under this condition, the noise attenuation of feedback architectures II and III is the same, regardless of feedback strength. Based on these results, we conclude that when pre-mRNA quickly decays, feedback architecture I will always provide better noise attenuation than feedback architecture II and III, as well as the no feedback case.

Next, we compare and contrast the feedback architectures based on the corresponding noise equations in the center column of Fig. 2 (not the limiting case in the rightmost column). Here, we investigate noise attenuation in relation to different species half-lives and pre-mRNA export rate. A species half-life is approximately equal to $ln(2)/\gamma_x$, where γ_x denotes the decay rate of species x.

First, in Fig. 4A, pre-mRNA decays faster than mRNA and protein. The ratio of pre-mRNA export and pre-mRNA decay, we denote as f, is held constant, thus pre-mRNA export (k_m) is also very fast. From this relationship, we conclude that when pre-mRNA has a faster decay rate, thus a shorter half-life, feedback architecture I always attenuates noise better than feedback to pre-mRNA decay (architecture II), feedback to pre-mRNA export (III), and the gene expression model without feedback. Next, we consider a condition when all rates of export and decay are similar. Fig. 4B depicts results of this condition, indicating that when feedback strength is low: inhibition of transcriptional bursting (feedback architecture I) and inhibition of mRNA export (feedback architecture III) exhibit similar noise attenuation, but as feedback strength increases: feedback architecture III attenuates noise best. Last, in Fig. 4C, we consider the case when protein has a long half life. This case resembles gene-expression featuring a very stable protein. Here, we conclude that feedback architecture I exhibits the greatest noise reduction for all feedback strengths.

VI. CONCLUSIONS

This paper explores possible regulatory motifs utilized by cells to reduce the inherent stochasticity of gene-expression. Explicit analytical expressions were developed to compare noise suppression of three possible feedback loops (Fig. IV). After investigation through mathematically controlled comparisons, it is discovered that the best feedback architecture is dependant on the various parameters associated with gene-expression. Transcriptional feedback (feedback architecture I) provides the best random noise regulation under the conditions of long protein half-life and also fast pre-mRNA export. When pre-mRNA export rate and species half-lives all occur at similar rates, negative feedback of pre-mRNA export (feedback architecture III) is best, although feedback architecture I has similar noise suppression abilities under this condition when feedback strength is low.

A. Relevance to Human Immunodeficiency Virus Type 1

Methods and findings from this paper can be applied to studying Human Immunodeficiency Virus type 1 (HIV-1). This virus undergoes a noise driven commitment decision between active replication or pro-viral latency [43], [44]. The later has been identified as the major obstacle in the way of finding a cure for HIV [45]. In this latent state, the cells become quiescent and unable to be identified, while maintaining the ability to become active at any time [46]. The long terminal repeat promoter in HIV-1 takes part in bursting events that contribute to the probabilistic fate selection of the virus. The feedback mechanisms explored in this work can further our insight of possible reduction of randomness by attenuating the noisy transcriptional bursting present in HIV that affects its commitment decisions and fate stability [32].

B. Future Work

Biological systems include time delays that alter stability by creating realistic oscillations in the system. Incorporation of these intrinsic delays will allow further investigation of noise suppression properties under more physiologically relevant conditions. Future work will include the addition of time delays to the gene-expression model proposed in this paper and resulting analysis of feedback strategies I-III performance.

ACKNOWLEDGMENT

This work was supported by National Science Foundation through grant ECCS–1711548 to AS.

REFERENCES

[1] W. J. Blake, M. Kaern, C. R. Cantor, and J. J. Collins, "Noise in eukaryotic gene expression," *Nature*, vol. 422, pp. 633–637, 2003.

[2] A. Bar-Even, J. Paulsson, M. Maheshri, E. Carmi, Y. P. OShea, and N. Barkai, "Noise in protein expression scales with natural protein abundance," *Nature*, vol. 38, pp. 636–643, 2006.

[3] S. M. Shaffer, M. C. Dunagin, S. R. Torborg, E. A. Torre, B. Emert, C. Krepler, M. Beqiri, K. Sproesser, P. A. Brafford, M. Xiao, E. Eggan, I. N. Anastopoulos, C. A. Vargas-Garcia, A. Singh, K. L. Nathanson, M. Herlyn, and A. Raj, "Rare cell variability and drug-induced reprogramming as a mode of cancer drug resistance," *Nature*, vol. 546, pp. 431–435, 2018.

[4] E. Libby, T. J. Perkins, and P. S. Swain, "Noisy information processing through transcriptional regulation," *Proceedings of the National Academy of Sciences*, vol. 104, pp. 7151–7156, 2007.

[5] H. B. Fraser, A. E. Hirsh, G. Giaever, J. Kumm, and M. B. Eisen, "Noise minimization in eukaryotic gene expression," *PLOS Biology*, vol. 2, p. e137, 2004.

[6] B. Lehner, "Selection to minimise noise in living systems and its implications for the evolution of gene expression," *Molecular Systems Biology*, vol. 4, p. 170, 2008.

[7] R. Kemkemer, S. Schrank, W. Vogel, H. Gruler, and D. Kaufmann, "Increased noise as an effect of haploinsufficiency of the tumor-suppressor gene neurofibromatosis type 1 in vitro," *Proceedings of the National Academy of Sciences*, vol. 99, pp. 13783–13788, 2002.

[8] D. L. Cook, A. N. Gerber, and S. J. Tapscott, "Modeling stochastic gene expression: implications for haploinsufficiency," *Proceedings of the National Academy of Sciences*, vol. 95, pp. 15641–15646, 1998.

[9] R. Bahar, C. H. Hartmann, K. A. Rodriguez, A. D. Denny, R. A. Busuttil, M. E. Dolle, R. B. Calder, G. B. Chisholm, B. H. Pollock, C. A. Klein, and J. Vijg, "Increased cell-to-cell variation in gene expression in ageing mouse heart," *Nature*, vol. 441, pp. 1011–1014, 2006.

[10] A. Brock, H. Chang, and S. Huang, "Non-genetic heterogeneity – a mutation-independent driving force for the somatic evolution of tumours," *Nature Reviews Genetics*, vol. 10, pp. 336–342, 2009.

[11] N. Balaban, J. Merrin, R. Chait, L. Kowalik, and S. Leibler, "Bacterial persistence as a phenotypic switch," *Science*, vol. 305, pp. 1622–1625, 2004.

[12] J. Feng, D. A. Kessler, E. Ben-Jacob, and H. Levine, "Growth feedback as a basis for persister bistability," *Proceedings of the National Academy of Sciences*, vol. 111, pp. 544–549, 2014.

[13] E. Maisonneuve, M. Castro-Camargo, and K. Gerdes, "(p)ppGpp controls bacterial persistence by stochastic induction of toxin-antitoxin activity," *Cell*, vol. 154, pp. 1140–1150, 2013.

[14] I. E. Meouche, Y. Siu, and M. J. Dunlop, "Stochastic expression of a multiple antibiotic resistance activator confers transient resistance in single cells," *Scientific Reports*, vol. 6, p. 19538, 2016.

[15] A. Singh and J. P. Hespanha, "Optimal feedback strength for noise suppression in autoregulatory gene networks," *Biophysical Journal*, vol. 96, pp. 4013–4023, 2009.

[16] H. El-Samad and M. Khammash, "Regulated degradation is a mechanism for suppressing stochastic fluctuations in gene regulatory networks," *Biophysical Journal*, vol. 90, pp. 3749–3761, 2006.

[17] A. Singh and J. P. Hespanha, "Evolution of autoregulation in the presence of noise," *IET Systems Biology*, vol. 3, pp. 368–378, 2009.

[18] I. Lestas, G. Vinnicombegv, and J. Paulsson, "Fundamental limits on the suppression of molecular fluctuations," *Nature*, vol. 467, pp. 174–178, 2010.

[19] P. S. Swain, "Efficient attenuation of stochasticity in gene expression through post-transcriptional control," *Journal of Molecular Biology*, vol. 344, pp. 956–976, 2004.

[20] J. M. Pedraza and J. Paulsson, "Effects of molecular memory and bursting on fluctuations in gene expression," *Science*, vol. 319, pp. 339–343, 2008.

[21] Y. Morishita and K. Aihara, "Noise-reduction through interaction in gene expression and biochemical reaction processes," *Journal of Theoretical Biology*, vol. 228, pp. 315–325, 2004.

[22] A. Singh, "Negative feedback through mrna provides the best control of gene-expression noise," *IEEE Transactions on NanoBioscience*, vol. 10, pp. 194–200, Sept 2011.

[23] A. Singh and J. P. Hespanha, "Reducing noise through translational control in an auto-regulatory gene network," in *2009 American Control Conference*, pp. 1712–1717, June 2009.

[24] M. M. Hansen, W. Y. Wen, E. Ingerman, B. S. Razooky, C. E. Thompson, R. D. Dar, C. W. Chin, M. L. Simpson, and L. S. Weinberger, "A post-transcriptional feedback mechanism for noise suppression and fate stabilization," *Cell*, 2018.

[25] T. Stoeger, N. Battich, and L. Pelkmans, "Passive noise filtering by cellular compartmentalization," *Cell*, vol. 164, pp. 1151–1161, 2016.

[26] N. Battich, T. Stoeger, and L. Pelkmans, "Control of transcript variability in single mammalian cells," *Cell*, vol. 163, pp. 1596–1610, 2015.

[27] M. M. Hansen, R. V. Desai, M. L. Simpson, and L. S. Weinberger, "Cytoplasmic amplification of transcriptional noise generates substantial cell-to-cell variability," *Cell*, vol. 7, pp. 384–387, 2018.

[28] A. Singh and P. Bokes, "Consequences of mRNA transport on stochastic variability in protein levels," *Biophysical Journal*, vol. 103, pp. 1087–1096, 2012.

[29] M. Sturrock, S. Li, and V. Shahrezaei, "The influence of nuclear compartmentalisation on stochastic dynamics of self-repressing gene expression," *Journal of Theoretical Biology*, vol. 424, pp. 55–72, 2017.

[30] N. Kumar, A. Singh, and R. V. Kulkarni, "Transcriptional bursting in gene expression: analytical results for general stochastic models," *PLOS Computational Biology*, vol. 11, p. e1004292, 2015.

[31] R. D. Dar, B. S. Razooky, A. Singh, T. V. Trimeloni, J. M. McCollum, C. D. Cox, M. L. Simpson, and L. S. Weinberger, "Transcriptional burst frequency and burst size are equally modulated across the human genome," *Proceedings of the National Academy of Sciences*, vol. 109, pp. 17454–17459, 2012.

[32] A. Singh, B. Razooky, C. D. Cox, M. L. Simpson, and L. S. Weinberger, "Transcriptional bursting from the HIV-1 promoter is a significant source of stochastic noise in HIV-1 gene expression," *Biophysical Journal*, vol. 98, pp. L32–L34, 2010.

[33] A. Raj, C. Peskin, D. Tranchina, D. Vargas, and S. Tyagi, "Stochastic mRNA synthesis in mammalian cells," *PLOS Biology*, vol. 4, p. e309, 2006.

[34] I. Golding, J. Paulsson, S. Zawilski, and E. Cox, "Real-time kinetics of gene activity in individual bacteria," *Cell*, vol. 123, pp. 1025–1036, 2005.

[35] D. M. Suter, N. Molina, D. Gatfield, K. Schneider, U. Schibler, and F. Naef, "Mammalian genes are transcribed with widely different bursting kinetics," *Science*, vol. 332, pp. 472–474, 2011.

[36] S. Yunger, L. Rosenfeld, Y. Garini, and Y. Shav-Tal, "Single-allele analysis of transcription kinetics in living mammalian cells," *Nature Methods*, vol. 7, pp. 631–633, 2010.

[37] P. Bokes, Y. Ting Lin, and A. Singh, "High cooperativity in negative feedback can amplify noisy gene expression," *Society for Mathematical Biology*, vol. 80, pp. 1871–1899, 2018.

[38] C. Fritzsche, S. Baumgartner, M. Kuban, D. Steinshorn, G. Reid, and S. Legewie, "Estrogendependent control and celltocell variability of transcriptional bursting," *Molecular Systems Biology*, vol. 14, 2018.

[39] M. A. Savageau, *Biochemical Systems Analysis: A Study of Function and Design in Molecular Biology*. Addison-Wesley, Reading, MA, 1976.

[40] J. P. Hespanha and A. Singh, "Stochastic models for chemically reacting systems using polynomial stochastic hybrid systems," *Int. J. Ro- bust Nonlinear Control*, vol. 15, pp. 669–689, 2005.

[41] A. Singh and J. P. Hespanha, "Approximate moment dynamics for chemically reacting systems," *IEEE Transactions on Automatic Control*, vol. 56, pp. 414–418, 2011.

[42] N. Van Kampen, *Stochastic processes in physics and chemistry*. Elsevier, 2011.

[43] A. Singh and L. S. Weinberger, "Stochastic gene expression as a molecular switch for viral latency," *Current Opinion in Microbiology*, vol. 12, pp. 460–466, 2009.

[44] L. S. Weinberger, J. Burnett, J. Toettcher, A. Arkin, and D. Schaffer, "Stochastic gene expression in a lentiviral positive-feedback loop: HIV-1 Tat fluctuations drive phenotypic diversity," *Cell*, vol. 122, pp. 169–182, 2005.

[45] D. D. Richman, "Introduction: challenges to finding a cure for HIV infection," *Current Opinion in HIV and AIDS*, vol. 6, pp. 1–3, 2011.

[46] A. Pai and L. Weinberger, "Fate-regulating circuits in viruses: From discovery to new therapy targets," *Annual Review of Virology*, vol. 4, no. 1, pp. 469–490, 2017.

Feedback Architecture	Gene Expression Noise (CV^2)	Gene Expression Noise (CV^2) (Limit as $\gamma_r \to \infty$)
	$CV^2 = \frac{\gamma_p(\gamma_m\gamma_p + \gamma_r(\gamma_m+\gamma_p)(1+f+B_ef) + \gamma_r{}^2(1+f)(1+f+B_ef))}{(\gamma_m+\gamma_p)(\gamma_r+\gamma_m+\gamma_r f)(\gamma_r+\gamma_p+\gamma_r f)\langle\bar{m}\rangle}$	$CV^2 = \frac{\gamma_p(1+f+B_ef)}{(\gamma_m+\gamma_p)(1+f)\langle\bar{m}\rangle}$
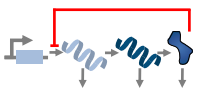	$CV^2{}_I = \frac{\gamma_p(\gamma_r(\gamma_m+\gamma_p)(1+f+B_ef) + \gamma_r{}^2(1+f)(1+f+B_ef) + \gamma_m\gamma_p(1+\varepsilon)}{((1+\varepsilon)((\gamma_m+\gamma_p)(\gamma_r+\gamma_m+\gamma_r f)(\gamma_r+\gamma_p+\gamma_r f) - \gamma_r\gamma_m\gamma_p(1+f)\varepsilon)\langle\bar{m}\rangle}$	$CV^2{}_I = \frac{\gamma_p(1+f+B_ef)}{(\gamma_m+\gamma_p)(1+f)(1+\varepsilon)\langle\bar{m}\rangle}$
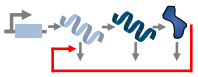	$CV^2{}_{II} = \frac{\gamma_p(\gamma_r(\gamma_m+\gamma_p)(1+f)(1+f+B_ef) + \gamma_r{}^2(1+f)^2(1+f+B_ef) + \gamma_m\gamma_p(1+f+\varepsilon)}{(1+f+\varepsilon)\left((\gamma_m+\gamma_p)(\gamma_r+\gamma_m+\gamma_r f)(\gamma_r+\gamma_p+\gamma_r f) - \gamma_r\gamma_m\gamma_p\varepsilon\right)\langle\bar{m}\rangle}$	$CV^2{}_{II} = \frac{\gamma_p(1+f+B_ef)}{(\gamma_m+\gamma_p)(1+f+\varepsilon)\langle\bar{m}\rangle}$
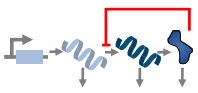	$CV^2{}_{III} = \frac{\gamma_p(\gamma_r(\gamma_m+\gamma_p)(1+f)(1+f+B_ef) + \gamma_r{}^2(1+f)^2(1+f+B_ef) + \gamma_m\gamma_p(1+f+\varepsilon)}{(1+f+\varepsilon)\left(\gamma_r(\gamma_m+\gamma_p)^2(1+f) + \gamma_r{}^2(\gamma_m+\gamma_p)(1+f)^2 + \gamma_r\gamma_m\gamma_p f\varepsilon + \gamma_m\gamma_p(\gamma_m+\gamma_p)(1+\varepsilon)\right)\langle\bar{m}\rangle}$	$CV^2{}_{III} = \frac{\gamma_p(1+f+B_ef)}{(\gamma_m+\gamma_p)(1+f+\varepsilon)\langle\bar{m}\rangle}$

Fig. 2: Steady-state average protein level noise of each feedback architecture is quantified by the coefficient of variation squared (CV_X^2) to enable comparison. The first column describes the form of feedback present: no feedback, (I) protein inhibition of its own transcription, (II) protein enhancing nuclear pre-mRNA decay, and (III) protein inhibition of pre-mRNA export. The center column contains the quantified average protein level noise equations. The rightmost column features a simplified version of the gene-expression noise equations, representing noise when the degradation of pre-mRNA is considered to be very fast and the ratio of pre-mRNA export and pre-mRNA degradation (f) is held constant. The parameters γ_r, γ_m, and γ_p denote the degradation of pre-mRNA, mRNA, and protein, respectively. The parameters f and B_e are described in (3). $\langle\bar{m}\rangle$ represents the steady state average of mRNA. ε represents the normalized feedback strength. Note that Poisson noise due to random births and deaths of protein molecules is ignored in these expressions.

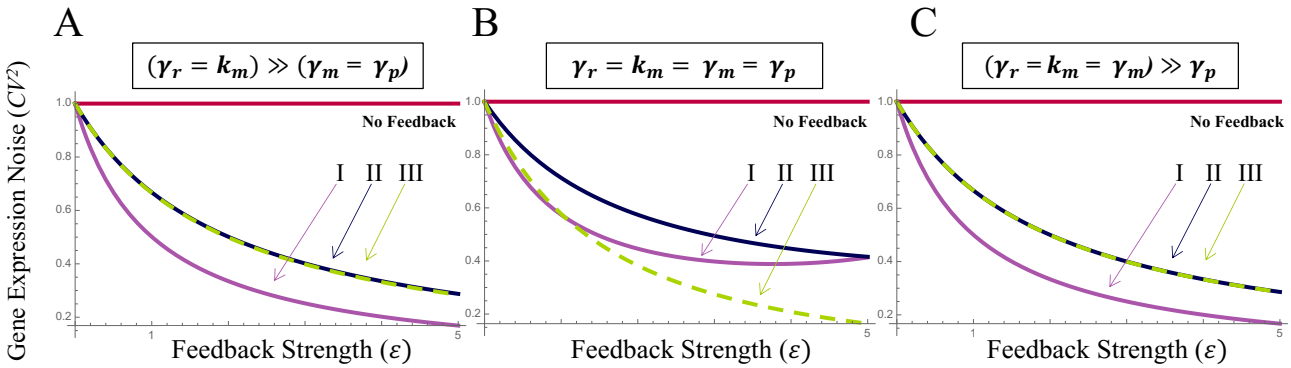

Fig. 4: Gene-expression noise (CV^2) of feedback architectures I-III are normalized by the case of no feedback. Noise is plotted as a function of increasing feedback strength. **(A)**: Plot A depicts gene-expression noise when pre-mRNA decay is much faster than mRNA decay and protein decay. Under this limit, feedback architecture I attenuates noise the best for all values of feedback strength, and feedback architectures II and III exhibit similar behavior. The parameters have the following values: γ_r = 10, γ_m = 1, γ_p = 1, f = 1, $\langle B_e\rangle$ = 10, and steady-state average number of mRNA molecules $\langle\bar{m}\rangle$ = 20. **(B)**: Plot B investigates noise attenuation when pre-mRNA export rate and species half-lives all have similar values. Here, feedback architecture I and III exhibit similar values of noise for low values of feedback strength, but at higher feedback strength, feedback architecture III is best. The parameters have the following values: γ_r = 1, γ_m = 1, γ_p = 1, f = 1, $\langle B_e\rangle$ = 10, and $\langle\bar{m}\rangle$ = 20. **(C)**: In plot C, protein decay rate is much less than pre-mRNA decay, pre-mRNA export, and mRNA decay rates. Here, feedback architecture I is best for all values of feedback strength ε. The parameters in the model consist of: γ_r = 1, γ_m = 1, γ_p = 0.01, f = 1, B_e = 10, and $\langle\bar{m}\rangle$ = 20.